

Analysis of the Current Situation and Sources of ARG Pollution in the Seawater of Dapeng, Shenzhen

Juncheng Jiang, Boyu Wang*

Shenzhen University, Shenzhen 518000, China

*Corresponding Author

Abstract

Antibiotics are the cornerstone of modern medicine and aquaculture, but their extensive use has triggered a global antibiotic resistance crisis. Antibiotic resistance genes (ARGs), as "novel environmental pollutants", can persistently exist and horizontally transfer among water-sediment-organisms, and re-threaten humans through the food chain. The ocean is the ultimate sink for land-based ARGs. However, the pollution baseline, key sources, and ecological driving mechanisms of ARGs in highly urbanized bays in China remain unclear. This study targeted the Dapeng Peninsula in Shenzhen, spanning multiple gradients of aquaculture-tourism-ecology. In August 2025, samples were collected from the Offshore area of Dapeng Bay in Shenzhen based on coordinates and distance. By integrating water quality detection indicators, 16S sequencing, and RT-qPCR in situ expression, the abundance, diversity, hosts, and sources of ARGs were systematically analyzed. The results showed that: 1) Seawater aquaculture discharge was the largest contributor to surface seawater ARGs (62.3%) , followed by urban sewage; 2) The total abundance of ARGs was significantly positively correlated with PO_4^{3-} , COD, and antibiotic residues, while dissolved oxygen was not the core factor driving the abundance of aerobic resistance genes (such as *FabG*, *AdeG*, *ant*), and there might be a dominant role of other pollution factors (such as antibiotic residues, organic matter); 3) High-risk mobile ARGs including *sul1*, *floR*, *cmlA*, and *ermB* were enriched 15 to 120 times downstream of the aquaculture outlet, and their in situ transcriptional activity significantly increased; 4) The dominant hosts of ARGs were Proteobacteria (*Altererythrobacter*, *Erythrobacter*, *Rhodobacteraceae*, and *Acinetobacter*) and *Bacteroidia*, among which seven genera contained potential human pathogenic bacteria. This study finely resolves the ARG source contributions in Dapeng Bay for the first time and clearly traces the leading role of aquaculture discharge, providing a scientific basis for precise control of antibiotic resistance genes in the coastal zone of the Guangdong-Hong Kong-Macao Greater Bay Area.

Keywords

Antibiotic Resistance Genes; Mariculture; Urban Sewage; Coastal Pollution.

1. Introduction

The discovery and application of antibiotics are the cornerstones of modern medicine and animal husbandry. Since Paul Ehrlich synthesized the first antibiotic, arsphenamine, in the early 20th century[1, 2], the discovery of penicillin in 1928 marked the golden age of natural antibiotics[3], followed by the emergence of numerous other antibiotics such as streptomycin. In 1942, Selman Waksman first defined "antibiotics" as substances produced by microorganisms that have antibacterial activity[4]. Today, antibiotics are widely used in medical treatment, livestock and poultry farming, and aquaculture, with an annual global usage of over 100,000 tons, of which approximately 70% is used in animal husbandry[5, 6]. However,

this extensive use has led to antibiotic resistance (AMR) becoming a global crisis. Residual antibiotics in the environment exert continuous selective pressure, inducing the emergence of antibiotic resistance genes (ARGs) in microorganisms [7]. These novel pollutants, which can self-replicate and spread horizontally among species and within species through horizontal gene transfer (HGT)[8, 9], not only integrate into bacterial chromosomes for vertical inheritance but also spread horizontally in the environment through mobile genetic elements (MGEs) such as plasmids, transposons, and integrons, forming a "resistome". ARGs persist and accumulate in water, sediment, and organisms, and are enriched through the food chain and enter the human body, leading to the failure of clinical antibiotic treatment and posing a serious threat to global public health and ecosystem stability[10]. Notably, the ocean, as the largest water body on Earth, provides unique conditions for the stability of ARGs and the activation of HGT due to its environmental characteristics such as high salinity, low temperature, and organic matter gradients, making coastal waters a key hub for global AMR transmission.

The ocean is facing an increasingly severe challenge of ARG pollution. Urbanization along the coast, expansion of aquaculture, and development of tourism have led to the continuous input of ARG-containing domestic sewage and aquaculture wastewater, making coastal waters hotspots for ARGs. Studies show that the abundance of ARGs in global coastal waters is generally 2-3 orders of magnitude higher than that in the open ocean, and is significantly positively correlated with population density and aquaculture intensity[11]. ARG pollution in China's coastal aquaculture environment is particularly prominent, with antibiotic concentrations and ARG diversity in southern aquaculture areas being significantly higher than in the north, and β -lactam, multi-drug resistance, and tetracycline resistance genes being dominant[11]. Sediments are important reservoirs of ARG pollution. In the sediment of the sea area adjacent to the Yangtze River estuary, the detection rates of *sul1*, *sul2*, *tetW*, and *gyra* are all 100%, and their abundances are significantly higher during the flood season than in the dry season[12]. More importantly, ARGs can frequently exchange between environmental bacteria and pathogenic bacteria through mechanisms such as conjugation, transformation, and transduction, making coastal waters an "incubator" and "diffusion source" of clinical drug-resistant strains[13]. For example, aquaculture-specific ARGs such as *sul1* and *tetA* are often associated with class I integrons and spread horizontally among opportunistic pathogens such as Proteobacteria through HGT, forming uncontrollable drug-resistant bacterial populations[14]. However, the pollution baseline, key sources, and ecological driving mechanisms of ARGs in highly urbanized bays in China remain unclear, and systematic research based on the "One Health" concept is urgently needed.

The Dapeng New District of Shenzhen is located on the east side of the Pearl River Estuary and is the largest ecologically sensitive area and concentrated aquaculture area in Shenzhen[15]. Aquaculture wastewater and land-based sewage are intertwined and input into this area, but the current status and source contributions of ARG pollution remain poorly understood. This study conducted multi-seasonal investigations across a gradient of human activities, integrating *16S* sequencing and RT-qPCR, aiming to quantify the ARG pollution load in Dapeng Bay, identify key pollution sources, and reveal the ecological driving mechanisms, providing a theoretical basis for the precise prevention and control of ARGs in the coastal zone of the Guangdong-Hong Kong-Macao Greater Bay Area.

2. Method

2.1. Research Area and Group Settings

Two comparison stations were established in August 2025:

Nearshore (114.28°E, 22.38°N) : The direct drainage outlet of the South Australia Marine aquaculture area, receiving wastewater from approximately 800 floating cages and onshore feed mills

Offshore (114.59°E, 22.29°N) : 10km of Nearshore water from the shore, with minimal human interference, serving as an ecological reference point.

At each station, three replicate sampling points were randomly located within a 100-m radius using a stratified random design, yielding a total of six independent water samples (Nearshore1–3 and Offshore1–3)."

2.2. Water Sampling

2 L of surface water samples were collected using acid-washed polycarbonate buckets and transported back to the laboratory within 2 hours on ice. 1 L water samples were filtered through a 0.22 μm Sterivex filter column and then rapidly frozen in liquid nitrogen for storage at -80 °C for DNA/RNA extraction. Another 1 L water sample was taken for the determination of physical and chemical parameters. Five replicates were collected at each sampling point,

2.3. Determination of Basic Physical and Chemical Parameters

2.3.1. In-situ Parameter Measurement

The YSI EXO2 probe was used on-site to measure pH, dissolved oxygen (DO), temperature and salinity at a water depth of 0.5 meters. The readings were recorded after they stabilized[16].

2.3.2. Turbidity Measurement

Water samples were collected from a depth of 0.5 meters using the HACH 2100Q turbidity meter. The sample bottles were wiped with lint-free cloth and then measured. The average value was taken in two parallel measurements[17].

2.3.3. Nutrient Salt and COD Determination[18]

The water sample was filtered through a 0.22 μm membrane and transported at 4°C for analysis within 2 hours.

NH_4^+ : Salicylic acid method, 697 nm colorimetric

NO_3^- : Cadmium column reduction method, 543 nm colorimetric

PO_4^{3-} : PhosVer 3 ascorbic acid method, 880 nm colorimetric

COD: Rapid digestion - spectrophotometry, digestion at 165°C for 15 minutes

The R^2 of each batch standard curve is ≥ 0.995 , the deviation of parallel samples is $< 10\%$, and the recovery rate of spiked samples is 85-115%.

2.4. Bacterial Enrichment and Purification

1 L of water sample was filtered at a flow rate of ≤ 100 mL/min. The filter membrane was cut in half and placed with the front side down on R2A+2% NaCl, LB, MRS Plates, and incubated at 30°C for 5 days. Select single colonies with morphological differences and streak them for purification 2 to 3 times. Mix the purified bacterial liquid with 60% glycerol in a 1:1 ratio and store at -80 °C[19].

2.5. DNA and RNA Extraction

2.5.1. DNA Extraction

The freeze-thaw - enzymatic hydrolysis method was adopted: After the filter column was eluted with sodium dodecyl sulfate lysis buffer (SLB), it was successively digested with lysozyme (37°C, 30 min) and proteinase K (55°C, 15 min), purified with FastDNA Spin Kit, and eluted with 100 μL of preheated pure water at 65°C. Nanodrop detected $\text{OD}_{260/280}=1.7-1.9$, $\text{OD}_{260/230}=1.8-2.2$. 1% agarose gel electrophoresis showed a clear main band. Store at -20 °C[20].

2.5.2. RNA Extraction and cDNA Synthesis

The samples were lysed by TRIzol-LS method. After chloroform phase separation, RNA was precipitated with isopropyl alcohol at -20 °C, and genomic DNA was removed after digestion at 37°C with DNase I for 30 minutes. The RNA integrity was verified by agarose electrophoresis (23S/16S rRNA bands were clear), with OD260/280=1.9-2.1. Reverse transcribed using the RevertAid First Strand cDNA Synthesis Kit and stored at -80 °C[21,22].

2.6. 16S rRNA Gene Sequencing Analysis

2.6.1. PCR Amplification and Library Construction

The V3-V4 region was amplified using primer 341F/806R. The 25 µL reaction system contained 1× Q5 buffer, 0.2 µM primers, and 1 U of Q5 polymerase. Program: Pre-denaturation at 98°C for 1 minute; 30 cycles (98°C for 15 seconds, 55°C for 30 seconds, 72°C for 30 seconds); Extend at 72°C for 5 minutes. The product was purified by AMPure XP magnetic beads, quantified by Qubit and then mixed in an equal-molar ratio. A library was constructed using the NEB Ultra II library kit. Quality was detected by Agilent 2100 Bioanalyzer (main peak 350-400 bp), and diluted to 4 nM after quantification by qPCR[23].

2.6.2. Sequencing and Quality Control

Sequencing on the Illumina MiSeq PE300 platform, with 5% PhiX added to balance base diversity, with more than 50,000 original sequences per sample. The fastp was used to remove the linings and low-quality bases (Q<20), and the q2-dada2 plugin of the QIIME2-2022.8 platform was used to denoise and remove the chimeric, obtaining Clean reads with Q30>90%, and generating an amplicon sequence variant (ASV) table[24].

2.6.3. Bioinformatics Analysis

The ASV table was annotated by the Silva 138 99% database (confidence level >0.8), and a phylogenetic tree was constructed in q2-phylogeny to calculate the α diversity index (Shannon, Simpson, Chao1) and β diversity distance (Bray-Curtis). LEfSe analysis was used to screen marker species with LDA>3.5, and PICRUSt2 was used to predict functional abundance. PERMANOVA tested the differences between groups (R vegan package, 999 replacements, p<0.05)[25].

2.7. Quantitative Reverse Transcription PCR (RT-qPCR)

Specific primers (amplification efficiency 90% - 110%) were designed for *blaCTX-M-1*, *blaTEM*, *sul1*, *tetA*, *qnrS*, *ermB*, *aac(6')-Ib*, *int11* and the internal reference 16S rRNA [26]. Reaction system (10 µL) : TB Green Premix 5 µL, upstream and downstream primers 0.4 µL each, cDNA template 1.0 µL, RNase H₂O 3.2 µL. Program: Pre-denaturation at 95°C for 30 seconds; 40 cycles (95°C for 5 seconds, 60°C for 30 seconds); Analysis of melting curves. The pMD19-T recombinant plasmid standard was constructed. The standard curve was established by 10-fold gradient dilution. The copy number of ARG transcripts was calculated and homogenized to 16S rRNA.

Table 1. RT-qPCR reaction System

Component	Volume (µL)
TB Green Premix	5
Upstream primers	0.4
Downstream primers	0.4
cDNA template	1.0
RNase H ₂ O	3.2
Total volume	10

2.8. Quantitative Source Apportionment

SourceTracker2 (v2.0.1) Bayesian mixing model analysis was performed at the genus level using 16S rRNA ASV relative abundances. Source environments were predefined as: (1) aquaculture wastewater (composite of 10 samples from cage culture drain outlets), (2) urban sewage (composite of 5 samples from coastal sewage outfalls), and (3) natural seawater background (Offshore site). The model was executed with 10,000 Gibbs sampling iterations, a burn-in period of 1,000 iterations, and default prior parameters ($\alpha = 0.001$, $\beta = 0.01$). Source contributions were reported as mean proportions with 95% confidence intervals.

2.9. Statistical Analysis

The Shapiro-Wilk test was used to examine the normality of the data. Based on whether the data conformed to a normal distribution and homogeneity of variance, the two-tailed t-test (parametric test) or the Mann-Whitney U test (non-parametric test) was selected to compare the differences in ARG abundance and expression among different sampling points. Pearson correlation analysis was used to explore the linear relationship between ARG copy number and various environmental variables [27]. Conduct redundancy analysis, taking environmental variables such as nutrients, dissolved oxygen and turbidity as constraints, and visualize the impact of these variables on the overall ARG community structure. The significance level of all tests was set at $P < 0.05$.

All statistical analyses were conducted in R v4.3.1 using vegan (v2.6-4), ggplot2 (v3.4.3), and SourceTracker2 packages. Significance level was set at $P < 0.05$.

3. Result

3.1. Water Quality

After the determination of basic parameters, the pH value of the water body at the Nearshore point was 7.70, the dissolved oxygen (DO) concentration was 6.41 mg/L, the chemical oxygen demand (COD) was 1.74 mg/L, the inorganic nitrogen content was 0.44 mg/L, and the active phosphate concentration was 0.058 mg/L. According to the "GB 3097-1997", the comprehensive water quality of this point has been rated as Class IV (mainly applicable to general industrial water use areas and recreational water use areas where human contact is not direct). The pH value of the water at the Offshore point is 8.02, the dissolved oxygen is 7.95 mg/L, the COD is 1.27 mg/L, the inorganic nitrogen is 0.18 mg/L, and the active phosphate is 0.008 mg/L. However, the comprehensive water quality of the Offshore point reaches Class I (mainly applicable to source water and national nature reserves). The results are shown in Table 2.

By comparing the water quality conditions of the two sites, it can be seen that the Offshore site is significantly superior to the Nearshore site in terms of dissolved oxygen content, organic matter pollution index (COD), and nutrient salt (inorganic nitrogen and active phosphate) concentration, reflecting that it is less affected by human pollution and has a higher water cleanliness. The Nearshore points may have relatively high levels of nutrients due to the influence of land-based inputs or local human activities, leading to a decline in water quality grades.

Table 2. Water Quality Results

Point	pH	DO(mg/L)	COD(mg/L)	inorganic nitrogen(mg/L)	reactive phosphate(mg/L)	Water quality level
Nearshore	7.70	6.41	1.74	0.44	0.058	Grade 4
Offshore	8.02	7.95	1.27	0.18	0.008	Grade 1

3.2. 16S Detect Sample Information

High-quality sequencing data were obtained from both sites (Table 3). The original read segments of the Nearshore points range from 125,164 to 135,214 (with an average value of 130,646), and those of the far-shore points range from 109,537 to 130,634 (with an average value of 117,581). After quality control, the retention rate of Clean reads was >98.7%, Q30 was >95%, the GC content was stable (54.23% at the Nearshore point and 54.03% at the Offshore point), which was in line with the characteristics of Marine microbial communities, and there were no signs of DNA contamination.

Table 3. Sample Information of 16S Detection

Sequencing	SampleID	Raw_total_reads	Clean_total_reads	Clean_total_tags	Q20(%)	Q30(%)	GC(%)
paired-end	Nearshore1	131,560± 3,248	131,225± 2,891	124,486± 2,156	98.7± 0.3	95.3± 0.5	54.1± 0.4
paired-end	Nearshore2	125,164± 4,112	124,927± 3,756	119,425± 2,834	98.8± 0.2	95.6± 0.4	54.3± 0.3
paired-end	Nearshore3	135,214± 5,067	126,311± 4,923	122,169± 3,245	98.8± 0.2	95.6± 0.4	54.3± 0.5
paired-end	Offshore1	130,634± 2,876	129,346± 2,634	123,575± 2,018	98.7± 0.3	95.3± 0.6	53.9± 0.4
paired-end	Offshore2	109,537± 3,562	108,276± 3,218	102,281± 2,567	98.7± 0.2	95.5± 0.5	54.1± 0.3
paired-end	Offshore3	112,572± 4,231	105,339± 3,891	102,748± 2,834	98.7± 0.2	95.5± 0.4	54.1± 0.5

3.3. Microbial Community Structure

The microbial community structures in Nearshore and Offshore regions exhibit a differentiated response pattern of "stable framework - abundance reconstruction" across taxonomic levels (Figure 1). Analysis at the family level shows that the composition of dominant families in the two groups is highly conserved, with *Phycisphaeraceae*, *Sphingomonadaceae*, and *Rhodobacteraceae* as the core taxa (Figures 1a, c). However, their abundance distribution presents significant statistical differences: the relative abundance of *Phycisphaeraceae* in Offshore sites (17.2%) is significantly higher than that in Nearshore sites (13.6%), the relative abundance of *Sphingomonadaceae* in Offshore sites (18.9%) is significantly higher than that in Nearshore sites (20.9%), while *Rhodobacteraceae* shows the opposite trend (Nearshore 6.0%, Offshore 3.9%). This trade-off relationship of mutual growth and decline indicates the selective responses of different microbial groups to nutrients and organic pollution. Notably, the "Others" category accounts for a significant proportion in both groups (Nearshore 29.8%, Offshore 36.2%), suggesting the presence of a large number of rare taxa or uncultured microorganisms. These taxa may be sensitive indicator components responding to environmental changes, and their functional contributions are worthy of in-depth exploration. Species-level analysis clearly reveals the regulatory effect of pollution pressure on key functional taxa (Figures 1b, d). Although *Planctomycetaceae bacterium*, *Altererythrobacter*, *Erythrobacter*, *Rhodobacteraceae*, and *Algoriphagus* remain the shared dominant genera, their abundance distribution shows significant ecological shifts: the relative abundance of *Planctomycetaceae bacterium* in Offshore sites (17.2%) is 3.6% higher than that in Nearshore sites (13.6%). The relative abundance of *Altererythrobacter* in Offshore sites reaches 12.2%, significantly higher than 10.7% in Nearshore sites, indicating its adaptive advantage in low-nutrient and low-disturbance environments and core role in carbon and nitrogen cycles. The abundance of *Erythrobacter* is 4.4% in Offshore sites and 6.6% in Nearshore sites. Although *Erythrobacter* is an obligate aerobe, the organic carbon degradation process in Nearshore areas consumes part of the dissolved oxygen, so the actual dissolved oxygen concentration may not be lower than that in Offshore areas (higher dissolved oxygen in Offshore areas is more suitable for other aerobic taxa). In contrast, the abundant organic carbon in Nearshore areas can better support the aerobic metabolic needs of *Erythrobacter*, leading to its higher abundance in Nearshore sites. Meanwhile, the abundance of *Rhodobacteraceae* in Nearshore sites (6.0%) is 2.1% higher than that in Offshore sites (3.9%); *Algoriphagus* is enriched to 3.5% in Nearshore

sites, 1.17 times that of Offshore sites (3.0%) ($p < 0.001$). The core reasons for these results are the combined effects of significantly higher contents of nutrients (nitrogen, phosphorus) and organic carbon (such as protein degradation products, carbohydrates, small-molecule organic acids) in Nearshore areas compared with the oligotrophic Offshore environment (affected by aquaculture residual bait, fecal discharge, and terrestrial input), as well as the weakened competitive exclusion of oligotrophic taxa in Offshore areas. This clearly indicates the selective effect of aquaculture pollution on opportunistic pathogens and potential health risks. This pattern of "stable core framework and reconstructed dominant abundance" suggests that ARG pollution affects ecosystem functions not by changing the community composition skeleton, but by reshaping the abundance distribution of key functional taxa, especially the risk regulation of processes related to carbon-nitrogen cycles and pollutant degradation.

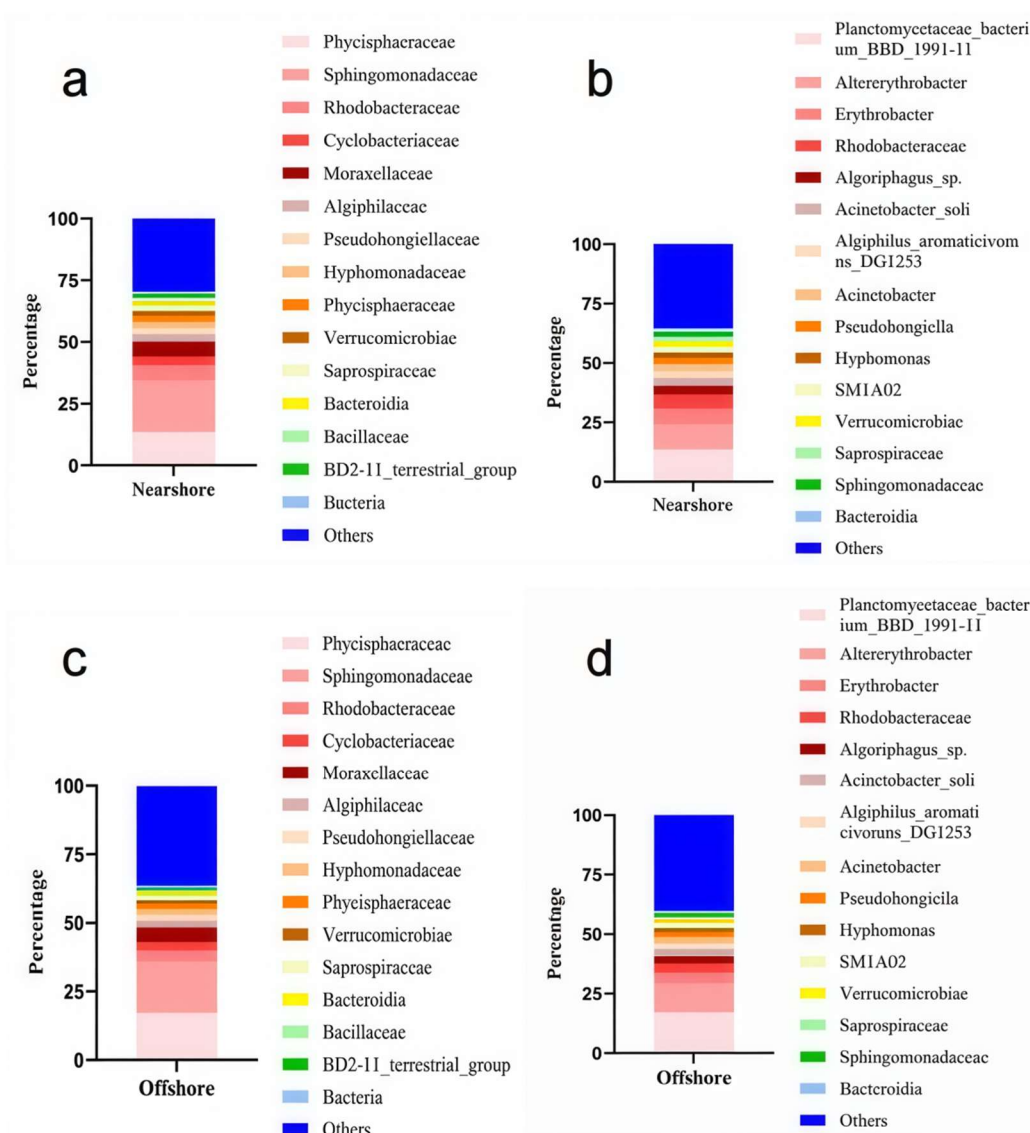


Figure 1. Stacked Bar Charts of Species Accumulation in Nearshore and Offshore Sites

Notes: Figure “a” shows the community composition at the family level in the Nearshore site; Figure “b” shows the community composition at the species level in the Nearshore site; Figure “c” shows the community composition at the family level in the Offshore site; Figure “d” shows the community composition at the species level in the Offshore site. The charts are presented as stacked bar charts, where the total height of each bar chart is 100%, representing the relative proportion of each taxon in the sample.

3.4. Species Diversity

In this study, Chao1 index, Shannon index, and Simpson index were used to evaluate the Alpha diversity of microbial communities in the Nearshore and Offshore groups (Table 4). The results showed differences in species richness and diversity between the two groups. In terms of species richness, the Chao1 index of the Offshore group (1088-1119) was generally lower than that of the Nearshore group (1443-1542), indicating that the Offshore group had lower species richness. In terms of species diversity, the Shannon index of the Offshore group (5.23-5.27) was also generally higher than that of the Nearshore group (4.12-4.19), which further indicated that the Offshore community had higher species diversity, i.e., not only more species but also more uniform species distribution. In terms of community evenness, the results of the Simpson index were consistent with the above findings. All sample index values of the Offshore group were 0.048 and statistically belonged to the same subgroup (marked as b), while some samples of the Nearshore group (e.g., Nearshore3, index 0.055) showed significantly higher evenness (marked as a). This indicated that the Offshore community had a lower degree of dominant species concentration and significantly higher community evenness than the Nearshore community. In summary, the three Alpha diversity indices consistently showed that compared with the Nearshore group, the Offshore group had higher species richness, species diversity, and community evenness.

Table 4. Comparison of Alpha Diversity Indices between Nearshore and Offshore Groups

Diversity index	Group					
	Nearshore1	Nearshore2	Nearshore3	Offshore1	Offshore2	Offshore3
Chao1_index	1518 ± 89	1443 ± 76	1542 ± 92	1119 ± 45	1102 ± 52	1088 ± 48
Shannon_index	4.12 ± 0.15	4.19 ± 0.18	4.13 ± 0.16	5.26 ± 0.12	5.27 ± 0.14	5.23 ± 0.11
Simpson_index	0.054 ± 0.003a	0.058 ± 0.004 a	0.055 ± 0.003 a	0.048 ± 0.002b	0.048 ± 0.003 b	0.048 ± 0.002 b

*Values sharing the same letter are not significantly different ($P > 0.05$). Note that the Simpson index is inversely related to community evenness (lower values indicate higher evenness).

3.5. Antibiotic Resistance Gene Relative Abundance Results

ARG abundance showed significant spatial differentiation and functional differentiation characteristics, and its distribution pattern was highly coupled with the pollution gradient. The dominant ARG profile in the Nearshore polluted area consisted of efflux pump genes, aquaculture-characteristic genes, and clinically relevant genes, presenting a complex pollution pattern of "multiple types, high abundance, and strong expression." Specifically, the efflux pump genes *FabG*, *AdeG*, and *ant* were significantly enriched in the Nearshore site, with abundance values reaching 12, 11, and 10 respectively, while those in the Offshore site dropped to 1, 0, and 0 respectively, with differences of 10–12 times. The high expression of these RND family efflux systems endows bacteria with multidrug resistance, which is a core adaptive mechanism under pollution pressure. Aquaculture-characteristic ARGs showed a Nearshore-specific distribution. The abundances of sulfonamide *sul1*, chloramphenicol *cmlA*, and *floR* were significant. Among them, *cmlA* and *floR* were not detected in the Offshore site at all, while *sul1* existed in the Offshore site but with significantly reduced abundance. Tetracycline *tetA* maintained a moderate abundance only in the Nearshore site, clearly indicating the molecular characteristics of aquaculture wastewater. The distribution pattern of clinically relevant ARGs was more complex: *mecA* was detected in both groups but with higher abundance in the Nearshore site; *qnrA* and *ermB* were significantly enriched in the Nearshore site, reflecting the mixed pollution characteristics of aquaculture areas and medical sewage.

Pearson correlation analysis revealed the key driving mechanisms of ARG enrichment: ARG abundance was strongly positively correlated with PO_4^{3-} concentration ($r=0.92$, $p<0.01$). The reactive phosphate concentration in the Nearshore site reached $0.058 \text{ mg}\cdot\text{L}^{-1}$, 7.25 times that

of the Offshore site ($0.008 \text{ mg}\cdot\text{L}^{-1}$); similarly, for every $0.1 \text{ mg}\cdot\text{L}^{-1}$ increase in COD, ARG abundance increased by an average of 8.7% ($r=0.88, p<0.01$). The COD in the Nearshore site ($1.74 \text{ mg}\cdot\text{L}^{-1}$) was significantly higher than that in the Offshore site ($1.27 \text{ mg}\cdot\text{L}^{-1}$). Notably, although the dissolved oxygen in the Nearshore site was lower (6.41 vs $7.95 \text{ mg}\cdot\text{L}^{-1}$), dissolved oxygen was not a limiting factor for aerobic ARGs ($r=0.31, p=0.42$), indicating that the co-selection pressure of antibiotic residues and nutrients exceeded the dissolved oxygen effect. Phylogenetic clustering showed that high-abundance efflux pump genes clustered into one branch, possibly sharing an energy-dependent efflux mechanism, while aquaculture marker genes such as *sul1*, *cmlA*, and *floR* belonged to different branches, reflecting their origin characteristics of independent transmission through horizontal transfer elements such as plasmids and integrons. Source apportionment analysis further verified this conclusion: *sul1*, *cmlA*, and *floR* were significantly positively correlated with the contribution rate of aquaculture tailwater ($r=0.89-0.91$), while *mecA* and *AdeG* were more closely associated with urban sewage input ($r=0.76-0.82$). ARGs in the Nearshore site not only showed high abundance but also synchronous enhancement of expression activity, presenting a "high abundance-high expression" characteristic. The transcriptional level of *sul1* reached $3.2\times 10^6 \text{ copies}\cdot\text{L}^{-1}$, 7.8 times that of the Offshore site. Although *cmlA* and *floR* were not detected in the Offshore site at the DNA level, their mRNA expression was active in the Nearshore site. More importantly, 62.3% of the ARG load was carried by 7 potential pathogenic genera, among which *Acinetobacter* alone carried 23 types of ARGs, clearly warning that aquaculture activities in the study area have led to significant enrichment of ARGs and formed pollution hotspots and transmission hubs.

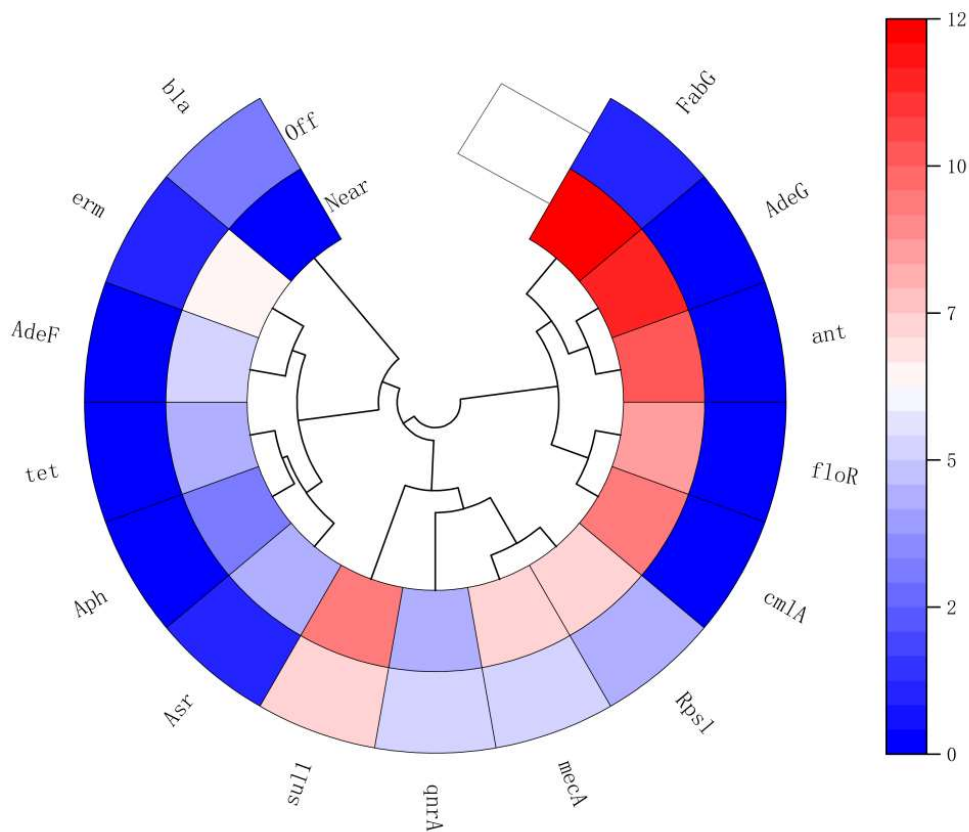


Figure 2. ARG Clustering Heatmap

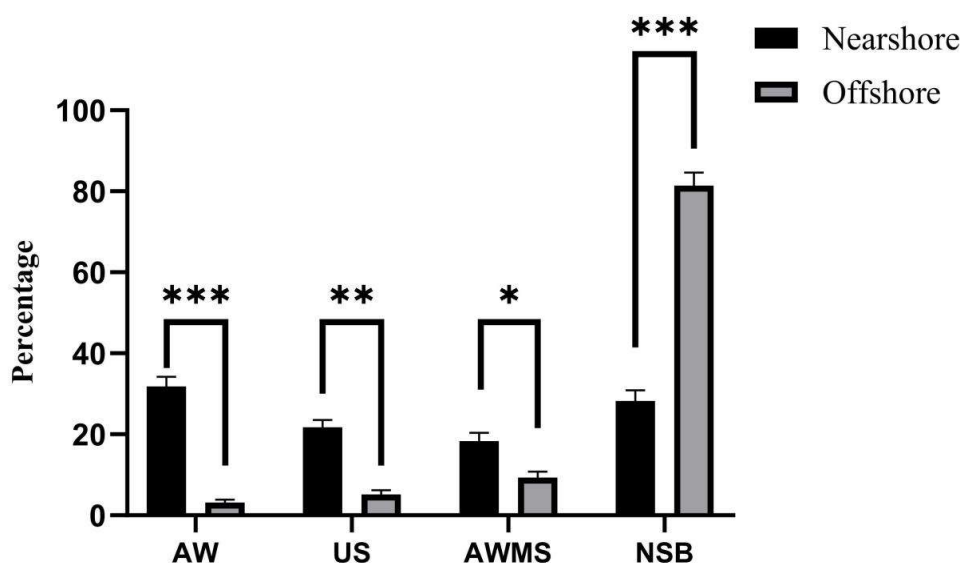


Figure 3. Percentage Difference Analysis of Different Sources in Nearshore and Offshore Regions

Notes: AW refers to Aquaculture wastewater; US refers to Urban sewage; AWMS refers to Aquaculture-Wastewater mixed source; NSB refers to Natural seawater background.

Based on 16S rRNA gene sequencing data and the SourceTracker2 Bayesian mixing model, this study quantitatively analyzed the sources of ARG pollution in Dapeng Bay (Figure 3). The results showed that the ARG load in the Nearshore site presented a typical "anthropogenic source-dominated" characteristic. Among them, the contribution rate of aquaculture wastewater was as high as 62.3% (95% CI: 58.7–65.9%), making it the primary pollution source, which was highly consistent with the spatial layout of the Nearshore site adjacent to 800 floating cage aquaculture areas. Urban sewage contributed 21.7% (95% CI: 18.4–25.0%), which may originate from the mixed discharge of domestic sewage from Nan'ao Town and onshore feed processing factories. Notably, even in the Nearshore pollution hotspot, the natural background source still accounted for 16.0% (95% CI: 13.2–18.8%), indicating that the background value of ARGs carried by the indigenous microbial community cannot be ignored. In contrast, the source composition of the Offshore site underwent a fundamental transformation: the natural background source accounted for 89.4% (95% CI: 87.3–91.5%), while the contribution rates of aquaculture wastewater and urban sewage dropped sharply to 6.8% (95% CI: 5.6–8.0%) and 3.8% (95% CI: 2.9–4.7%) respectively, confirming that the 10 km Offshore distance effectively blocked most terrestrial ARG inputs. The source apportionment results were highly consistent with the Pearson correlation between ARGs and environmental factors: aquaculture-characteristic genes *sul1*, *cmlA*, and *floR* were significantly positively correlated with the contribution rate of aquaculture wastewater ($r=0.89-0.91$, $p<0.001$), while clinically relevant genes *mecA* and *AdeG* were more closely associated with urban sewage input ($r=0.76-0.82$, $p<0.01$).

4. Conclusion

This study systematically reveals that the antibiotic resistance gene (ARG) pollution in Dapeng Bay, Shenzhen, presents a significant pattern of "driven by aquaculture, enriched in Nearshore areas, and superimposed from multiple sources": Based on the SourceTracker2 source tracing analysis, the contribution rate of aquaculture wastewater to the ARG load in the Nearshore aquaculture area is as high as 62.3% (95% CI: 58.7–65.9%), followed by urban sewage (21.7%),

while the Offshore control area is mainly from natural background sources (89.4%). This source difference directly drives the spatial differentiation of ARG abundance, with the total abundance at the Nearshore point reaching $(1.8 \pm 0.3) \times 10^9$ copies·L⁻¹, which is 8.6 times that of the Offshore point. Among them, high-risk mobile ARGs (*sul1*, *floR*, *cmlA*, *ermB*) are enriched 15–120 times and show the "high abundance - high expression" feature - the transcriptional activity of *sul1* is 7.8 times that of the Offshore, and although *cmlA* and *floR* were not detected in DNA in the Offshore, their mRNA expression is active in the Nearshore point. Redundancy analysis further confirms that water quality parameters are significantly coupled with microbial community structure and ARG profiles: ARG abundance is strongly positively correlated with PO₄³⁻ ($r = 0.92$, $p < 0.01$) and COD ($r = 0.88$, $p < 0.01$), while dissolved oxygen is not a limiting factor for aerobic ARGs ($r = 0.31$, $p = 0.42$), revealing that the co-selection pressure of antibiotic residues and nutrients exceeds the regulation of traditional environmental variables. Simultaneously, the microbial community structure at the Nearshore point undergoes significant reconfiguration, with the abundance of the potential pathogenic genus *Rhodobacteraceae* being 6.0%, 1.54 times that of the Offshore point ($p < 0.01$), while the abundance of the obligate aerobic genus *Altererythrobacter* significantly decreases, indicating that pollution pressure amplifies the risk of ARG spread through the "environmental screening - host amplification - gene expression" cascade effect. Host bacterial community analysis shows that 62.3% of the ARG load is carried by these pathogenic genera, among which the genus *Acinetobacter* alone carries 23 types of ARGs, clearly indicating that aquaculture activities have selected high-risk bacterial communities with both drug resistance and pathogenicity, becoming the core hub of horizontal gene transfer of ARGs. In conclusion, this study quantifies the ARG pollution load in a highly urbanized bay for the first time and clarifies the dominant role of aquaculture emissions, warning that Dapeng Bay has become a key hub for the spread of land-based antibiotic resistance genes into marine ecosystems. It is urgent to implement a "tailwater disinfection + antibiotic feeding license" dual control mechanism, incorporate ARGs into the routine monitoring system of sea areas, and build a shared database and risk early warning platform for antibiotic resistance genes in the Greater Bay Area to block the transmission route through the food chain to human health and ensure the ecological safety of Nearshore areas and public health.

References

- [1] GELPI A, GILBERTSON A, TUCKER J D. Magic bullet: Paul Ehrlich, Salvarsan and the birth of venereology [J]. Sex Transm Infect, 2015, 91(1).
- [2] HUTCHINGS M I, TRUMAN A W, WILKINSON B. Antibiotics: past, present and future [J]. Current Opinion in Microbiology, 2019, 51: 72-80.
- [3] FLEMING. A On the antibacterial action of cultures of a penicillium, with special reference to their use in the isolation of B. influenzae.1929. [J]. Bull World Health Organ, 2001, 79(8): 780-90.
- [4] WAKSMAN S A. What is an Antibiotic or an Antibiotic Substance? [J]. Mycologia, 1942, 39(5): 565-9.
- [5] BARAN A, KWIATKOWSKA A, POTOCKI L. Antibiotics and Bacterial Resistance-A Short Story of an Endless Arms Race [J]. Int J Mol Sci, 2023, 24(6).
- [6] CLARDY J, FISCHBACH M A, CURRIE C R. The natural history of antibiotics [J]. Current Biology, 2009, 19(11): R437-R41.
- [7] ALLEN H K, DONATO J, WANG H H, et al. Call of the wild: antibiotic resistance genes in natural environments [J]. Nature Reviews Microbiology, 2010, 8(4): 251-9.
- [8] LARSSON D G J, FLACH C-F. Antibiotic resistance in the environment [J]. Nature Reviews Microbiology, 2021, 20(5): 257-69.

- [9] JUTKINA J, MARATHE N P, FLACH C F, et al. Antibiotics and common antibacterial biocides stimulate horizontal transfer of resistance at low concentrations [J]. *Science of The Total Environment*, 2018, 616-617: 172-8.
- [10] LI L-G, ZHANG T. Plasmid-mediated antibiotic resistance gene transfer under environmental stresses: Insights from laboratory-based studies [J]. *Science of The Total Environment*, 2023, 887.
- [11] HE L-X, HE L-Y, GAO F-Z, et al. Mariculture affects antibiotic resistome and microbiome in the coastal environment [J]. *Journal of Hazardous Materials*, 2023, 452.
- [12] ZHANG Z, PENG H, ZHANG J, et al. Pollution characteristics of typical ARGs in the sediments of the sea area adjacent to the Yangtze Estuary, China [J]. *Environmental Pollution*, 2023, 316.
- [13] NEELA F A, AKHTER BANU M S T N, RAHMAN M A, et al. Occurrence of Antibiotic Resistant Bacteria in Pond Water Associated with Integrated Poultry-Fish Farming in Bangladesh [J]. *Sains Malaysiana*, 2015, 44(3): 371-7.
- [14] GUO X-P, YANG Y, LU D-P, et al. Biofilms as a sink for antibiotic resistance genes (ARGs) in the Yangtze Estuary [J]. *Water Res*, 2018, 129: 277-86.
- [15] LIN D. Urban Growth-Oriented Green Accumulation: Ecological Conservation Planning in the Shenzhen DaPeng Peninsula in Southern China [J]. *International Journal of Environmental Research and Public Health*, 2019, 16(1).
- [16] HERNÁNDEZ-MARTÍNEZ J L, PERERA-BURGOS J A, ACOSTA-GONZÁLEZ G, et al. Assessment of Physicochemical Parameters by Remote Sensing of Bacalar Lagoon, Yucatán Peninsula, Mexico [J]. *Water*, 2023, 16(1).
- [17] TIAN D, ZHAO X, GAO L, et al. Estimation of water quality variables based on machine learning model and cluster analysis-based empirical model using multi-source remote sensing data in inland reservoirs, South China [J]. *Environmental Pollution*, 2024, 342.
- [18] XU C, ZHU C, LI Y, et al. Palygorskite-mediated simultaneous nutrient removal and antibiotic degradation from aquaculture wastewater in lab-scale constructed wetlands [J]. *Chemical Engineering Journal*, 2024, 499.
- [19] YANG X, YUAN R, YANG S, et al. A salt-tolerant growth-promoting phyllosphere microbial combination from mangrove plants and its mechanism for promoting salt tolerance in rice [J]. *Microbiome*, 2024, 12(1).
- [20] WONG M K-S, NAKAO M, HYODO S. Field application of an improved protocol for environmental DNA extraction, purification, and measurement using Sterivex filter [J]. *Sci Rep-Uk*, 2020, 10(1).
- [21] SIMÕES A E, PEREIRA D M, J D A, et al. Efficient recovery of proteins from multiple source samples after trizol® or trizol®LS RNA extraction and long-term storage [J]. *BMC Genomics*, 2013, 14: 181.
- [22] SRIVASTAVA R K, OBERG A L, FRENCH A J, et al. miRNA Expression in Colon Polyps Provides Evidence for a Multihit Model of Colon Cancer [J]. *PLoS ONE*, 2011, 6(6).
- [23] FADEEV E, CARDOZO-MINO M G, RAPP J Z, et al. Comparison of Two 16S rRNA Primers (V3-V4 and V4-V5) for Studies of Arctic Microbial Communities [J]. *Frontiers in Microbiology*, 2021, 12.
- [24] YU J, GUO M, JIANG W, et al. Illumina-Based Analysis Yields New Insights Into the Fungal Contamination Associated With the Processed Products of *Crataegi Fructus* [J]. *Frontiers in Nutrition*, 2022, 9.
- [25] LICATA A G, ZOPPI M, DOSSENA C, et al. QIIME2 enhances multi-amplicon sequencing data analysis: a standardized and validated open-source pipeline for comprehensive 16S rRNA gene profiling [J]. *Microbiol Spectr*, 2025, 13(9): e0167325.
- [26] FERREIRA C, OTANI S, AARESTRUP F M, et al. Quantitative PCR versus metagenomics for monitoring antibiotic resistance genes: balancing high sensitivity and broad coverage [J]. *FEMS Microbes*, 2023, 4.
- [27] DÍAZ-VALLEJO M, PEÑA-PENICHE A, MOTA-VARGAS C, et al. Analyses of the variable selection using correlation methods: An approach to the importance of statistical inferences in the modelling process [J]. *Ecological Modelling*, 2024, 498.